Targeted Discovery of Tetrapeptides and Cyclic Polyketide-Peptide Hybrids from a Fungal Antagonist of Farming Termites

Felix Schalk[+],[a] Soohyun Um[+],[a] Huijuan Guo,[a] Nina B. Kreuzenbeck,[a] Helmar Görls,[b] Z. Wilhelm de Beer,[c] and Christine Beemelmanns*[a]

Dedicated to Prof. Rolf Huisgen.

Herein, we report the targeted isolation and characterization of four linear nonribosomally synthesized tetrapeptides (pseudoxylaramide A–D) and two cyclic nonribosomal peptide synthetase-polyketide synthase-derived natural products (xylacremolide A and B) from the termite-associated stowaway fungus *Pseudoxylaria* sp. X187. The fungal strain was prioritized for further metabolic analysis based on its taxonomical position and morphological and bioassay data. Metabolic data were dereplicated based on high-resolution tandem mass spectrometry data and global molecular networking analysis. The structure of all six new natural products was elucidated based on a combination of 1D and 2D NMR analysis, Marfey's analysis and X-ray crystallography.

Introduction

Termites of the subfamily Macrotermitinae grow a single species of a mutualistic fungus as food source.[1] Despite the dominating monocultural system,[2] species of the genus *Xylaria* (Ascomycota: Xylariaceae) are inconspicuously present within the comb.[3] Once growth conditions become more favorable within an aging or dying termite colony, germination and growth of *Pseudoxylaria* is initiated within the fungal garden, causing the displacement and repression of any remains of the fungal mutualist within days. Although it is as yet unclear how *Pseudoxylaria* senses a favorable environment, we hypothesize that *Pseudoxylaria*-derived secondary metabolites assist in the repression of the fungal mutualist.[4] Based on antagonistic behavior and the fact that Xylariaceae in general have been the source of a wide range of bioactive compounds,[5] we set out to gain deeper insights into the metabolic capacities of this subgenus. Based on its phylogenetic distinct position, we decided to focus on the strain named *Pseudoxylaria* sp. X187 and apply a high-resolution tandem mass spectrometry (HRMS) based approach to identify chemical features unique to this *Pseudoxylaria* species. Here, we report on the isolation of four linear nonribosomally (NRPS) synthesized peptides and two cyclic NRPS-polyketide synthase (PKS)-derived natural products.

Results and Discussion

In a first step, five *Pseudoxylaria* strains were isolated from termite mounds in South Africa and grown on PDA agar plates (21 days, 23 °C). Clean fungal hyphae were placed on fresh PDA plates and sub-cultured to obtain a pure isolate. To determine the identity of the fungal strain, a partial sequence from the ribosomal DNA (rDNA) and the internal transcribed spacer region (ITS, primer ITS1 5′-TCCGTAGGTGAACCTGCGG-3′ and ITS4 5′-TCCTCCGCTTATTGATATGC-3′) was sequenced and compared to a phylogenetic framework (Figure S1 in the Supporting Information). Based on its distinct phylogenetic position, fast growth and moderate antimicrobial activity (Figures S1 and S2, Table S7) *Pseudoxylaria* sp. X187 was selected for a more detailed metabolic analysis using liquid chromatography (LC) coupled with HRMS^2 measurements. The resulting data set was then subjected to global natural products social molecular networking analysis (GNPS),[6] a powerful tool to process tandem mass spectrometry (MS^2) data. During cultivation of X187, we observed that aging of X187 (> 14 days) resulted in the regular exudation of droplets (guttation) within the older mycelium parts, which are known to be enriched in water-

[a] F. Schalk,[+] S. Um,[+] H. Guo, N. B. Kreuzenbeck, Dr. C. Beemelmanns
Chemical Biology of Microbe – Host Interactions
Institution Leibniz Institute for Natural Product Research and Infection Biology
Hans Knöll Institute (HKI)
Beutenbergstrasse 11a, 07745 Jena (Germany)
E-mail: christine.beemelmanns@hki-jena.de
[b] Dr. H. Görls
Institute for Inorganic and Analytical Chemistry
Friedrich-Schiller-University
Lessingstrasse 8, 07743 Jena (Germany)
[c] Prof. Z. W. de Beer
Department of Biochemistry, Genetics and Microbiology
Forestry and Agricultural Biotechnology Institute (FABI)
University of Pretoria
Hatfield, 0002, Pretoria (South Africa)
[+] These authors contributed equally to this work.

Supporting information for this article is available on the WWW under https://doi.org/10.1002/cbic.202000331

This article is part of a Special Collection on Microbial Biosynthesis and Interactions. To view the complete collection, visit our homepage

soluble metabolites including nutrients and bioactive compounds, but are generally depleted of media components.[7] Thus, guttation droplets were separately collected for detailed HRMS^2-based analysis of the X187-specific secretome.

As hypothesized, the comparative analysis of HRMS data retrieved from guttation droplets and crude culture extracts revealed a distinct and prominent MS^2 pattern within samples from guttation droplets and contained only very few annotated chemical features (Figure 1). Although extracts retrieved from full plate cultures contained to a certain extent the same uncharacterized MS^2 networks as found for the secreted droplets, additional subnetworks corresponding to primary metabolites, in particular phospholipids and fatty acids were detectable (Figure S2).

We were particularly intrigued by two extensive *m/z* subnetworks containing nine and 14 connected nodes with protonated molecular ions (*m/z* 623.3776 (**1**), *m/z* 609.3627 (**2**), *m/z* 657.3617 (**3**), *m/z* 643.3466 (**4**), *m/z* 403.2220 (**5**), *m/z* 417.2383 (**6**)). Dereplication of exact masses by using Antibase[8] and SciFinder indicated that the corresponding *m/z* signals might represent as yet unreported metabolites.

For structure elucidation of potentially novel compounds, we performed larger scale cultivating of X187 on PDA (400 mL, 10 plates, 150×16 mm) for a maximum of four weeks (optimal 28 days, indicated by strong droplet formation). To maximize yields, guttation droplets were separated from mycelium and separately purified. The remaining plates covered with fungal mycelium were cut into small pieces and extracted with MeOH using a previously established procedure.[4] Both extracts were purified and fractionated using a SPE C_{18} cartridge followed by MS-guided semi-preparative reversed-phase HPLC (phenyl-hexyl column), which resulted in the isolation and characterization of compounds (**1**–**6**) with matching HRMS and UV spectra from GNPS analysis.

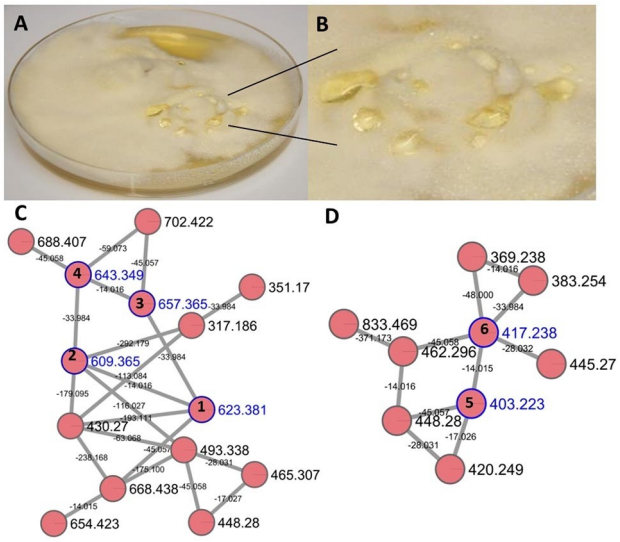

Figure 1. A) *Pseudoxylaria* sp. X187 with guttation droplets (PDA, 3 weeks) and B) enlarged picture of guttation droplets. C) Enlarged GNPS network cluster containing pseudoxylaramides A–D (**1**–**4**) and D) xylacremolides A and B (**5** and **6**).

First, we focused on the identification of the four major and potentially novel metabolites that were detected within the first MS^2 subnetwork (Figure 1C) and the total ion chromatograms (TIC) and showed each a unique molecular ion peak. MS-guided purification of enriched 80% methanol SPE fractions of culture extracts (Supporting Information) led to the isolation of the first major natural product **1** with the molecular formula $C_{35}H_{50}O_6N_4$ and thirteen degrees of unsaturation as determined by high-resolution mass spectrometry (HRMS (ESI) *m/z* $[M+H]^+$ calcd. for $C_{35}H_{51}O_6N_4^+$ 623.3803, found 623.3776, Δ_{ppm} −4.49) and NMR spectroscopy in [D_6]DMSO and CD_3OH (Table S3). The ^{13}C NMR spectrum exhibited typical analytical features of a peptide, which includes 20 amide/carboxylic acid carbonyl carbon signals and 20 α-carbon resonances, which was supported by ^1H NMR signals related to eight exchangeable amide proton signals. Analysis of ^1H and ^{13}C NMR data revealed that compound **1** exists as a set of four stable and inseparable conformations (in CD_3OH, ratio of ca. 10:7:3:2). The planar structure of pseudoxylaramide A (**1**) was assigned based on the distinct signal sets of the major isomer in CD_3OH. Interpretation of the COSY, HSQC and HMBC spectra indicated the presence of two *N*-methyl phenylalanine (*N*-Me–Phe) and two isoleucine residues. The connectivity of the four residues was established by analysis of the HMBC spectrum (Figure 2B). Correlations in the HMBC spectrum also revealed the presence of an *O*-methyl ester [δ_C 51.5; δ_H 3.68] at the C-terminal end of *N*-Me Phe1 [δ_C 170.8]. The *N*-methyl [δ_H 2.97] of *N*-Me Phe1 displayed clear correlations to C-2 [δ_C 59.0] and C-1′ [δ_C 172.4] confirming the connectivity between *N*-Me Phe1 and Ile1. The NH [δ_H 7.52] of Ile1 showed a heteronuclear correlation to C-1‴ [δ_C 170.1] of Phe2. The *N*-methyl protons [δ_H 2.99] of Phe2 displayed correlations in the HMBC spectrum with C-1‴ [δ_C 173.2] of Ile2, establishing the sequence from Phe2 to Ile2. The amide proton [δ_H 8.07] of Ile2 showed the long-range coupling to the methyl group [δ_C 21.1] and the methyl protons [δ_H 1.88] showed correlation (HMBC) to carbonyl carbon [δ_C 171.4] in Ile2 deducing an OH group of Ile2 was substituted by a methyl group. To determine the absolute configurations of the α-carbon of the incorporated amino acids, an acid hydrolysis and Marfey's analysis[9] with L- and D-FDAA (1-fluoro-2,4-dinitrophenyl-L,D-alanine amide) were performed. After acid hydrolysis of **1** (1 h, 6 N HCl at 115 °C), the hydrolysate was derivatized with FDAA and analyzed by using UHPLC-MS, which indicated that compound **1** consisted exclusively of L-amino acids. Also, isoleucine in **1** was determined as L-Ile by comparison of retention times with derivatized authentic standards.[10] As energy barriers for amide bond rotation might range from 18 to 30 kcal/mol depending on the nature of the amide moiety,[11] we assume that compound **1** exists as a set of four stable amide isomers (*cis* and *trans*) caused by the N-terminal acetamide moiety and the amide group connecting Ile2 and Phe1. As indicated by MS^2-network analysis, a congener **2** of compound **1** lacking a CH_2 unit was detectable roughly in a 10:1 ratio (**1**:**2**; HRMS (ESI) *m/z* $[M+H]^+$ calcd. for $C_{34}H_{49}O_6N_4^+$ 609.3647, found 609.3627, Δ_{ppm} −3.28). Again, MS-guided purification, NMR-based structure elucidation and Marfey's based analysis revealed the structure of methyl ester **2**, which occurs as four

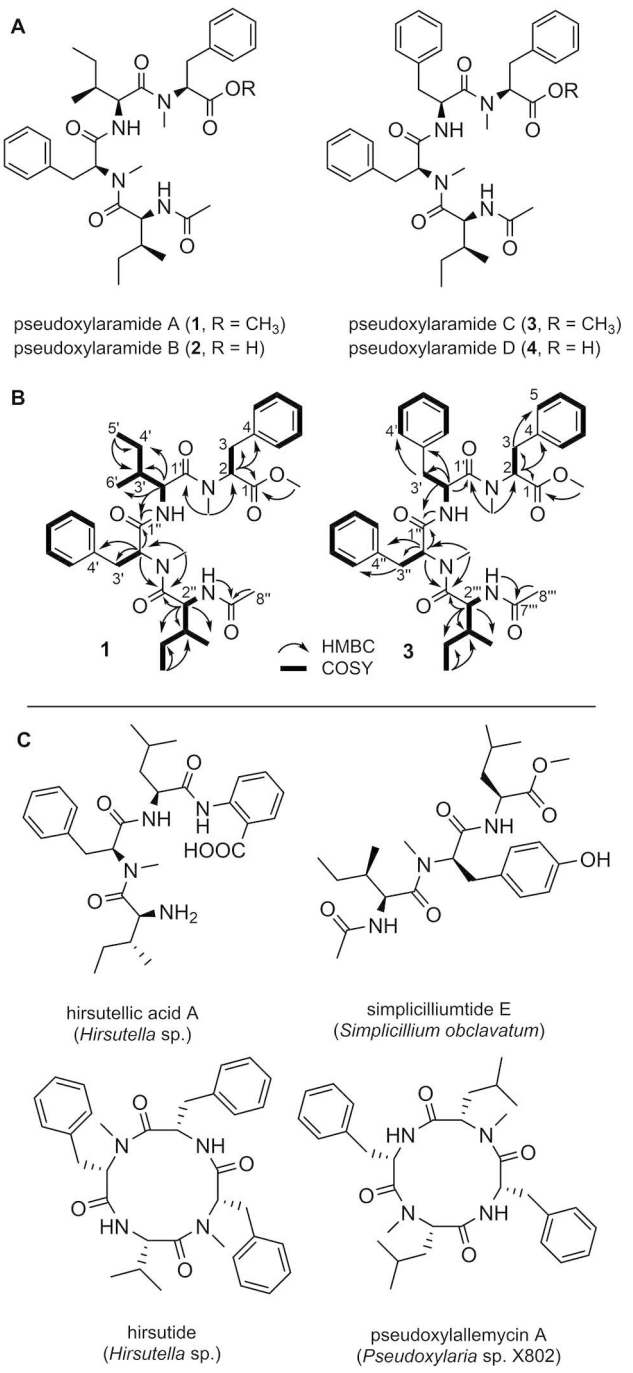

Figure 2. A) Structures of pseudoxylaramides A–D (**1**–**4**, shown as all-*trans* amide bond isomers) and B) key COSY and HMBC correlations (detectable from measurements in CD_3OH and $[D_6]DMSO$, respectively). C) Structures of related linear and cyclic fungal tetrapeptides.

inseparable amide isomers in a ratio of 10:6:5:3.5 in solution (CD_3OH). Based on their microbial origin, we named the linear peptides pseudoxylaramide A (**1**) and B (**2**) respectively. Following up on the MS^2-guided prediction, we then pursued an MS-guided analysis of the closely related molecular ions pseudoxylaramide C (**3**; HRMS (ESI) $[M+H]^+$ *m/z* calcd. for $C_{38}H_{49}O_6N_4^+$ 657.3647, found 657.3617, Δ_{ppm} −4.41) and pseudoxylaramide D (**4**; HRMS (ESI) *m/z* $[M+H]^+$ calcd. for $C_{37}H_{47}O_6N_4^+$ 643.3490, found 643.3466, Δ_{ppm} −3.90), which were assumed to be structural homologues containing a Phe moiety instead of Ile based on their MS^2 pattern and the deduced 17 degrees of unsaturation. Again, compound **3** was isolated as an inseparable mixture of four amide isomers in a ratio of 10:8:3:3 (CD_3OH), similar to compound **4** (isomeric ratio of 10:8.5:7:6 (CD_3OH)). Comparative 1D and 2D NMR analysis of all isolates (Table S4) revealed that pseudoxylaramide C (**3**) carried one Phe moiety instead of an Ile (**1**); a result which was confirmed by Marfey's analysis. Finally, pseudoxylaramide D (**4**) was identified as the free acid of **3**. Based on their homologous structural features, we named compound **3** and **4** pseudoxylaramides C (**3**) and D (**4**). Here, it is noteworthy that N-methylation in all four derivatives occurs solely at the first and third amide position (L-Phe). Based on the structural identification of compounds **1**–**4**, we reanalyzed the obtained MS^2 data and GNPS subnetwork and found that X187 presumably secretes minor amounts of tetrapeptide congeners that vary in the ratio of the two detected amino acids, Ile and Phe. Although detectable by $HRMS^2$, low production titers prevented further structure elucidation.

Compounds **1**–**4** share structural features with other linear tetrapeptides of fungal origin such as simplicilliumtides isolated from the marine fungus *Simplicillium obclavatum*,[12] and antimalarial hirsutellic acid from the entomopathogenic fungus *Hirsutella* sp. that infects spiders.[13] A similar N-methylation pattern (*N*-Me Phe) is also found in cyclized tetrapeptides, such as onychocin C from *Onychocola sclerotica*[14] and pseudoxylallemycin A isolated from *Pseudoxylaria* sp. X802 (Figure 2C).[6] Here it is important to note that the combination of N-methylation as well as N-acylation might prevent cyclization of the linear peptide as well as enzymatic degradation. Several structurally related tetrapeptides (linear and cyclic) were reported to have antimalarial or antibacterial activities. None of the isolated derivatives were active against our fungal and bacterial test strains and were thus not accountable for the observed activity of the crude extract of *Pseudoxylaria* sp. X187. Biosynthetically, pseudoxylaramides are likely produced by a tetramodular NRPS based on the collinearity principle commonly observed in both bacterial and fungal NRPSs.[15] As pseudoxylaramides dominantly consist of two pairs of amino acids, it is also possible that the tetrapeptides are biosynthesized by noncanonical NRPSs with functional domains that are capable of acting iteratively.[16] Future genomic and molecular biological studies on *Pseudoxylaria* are now directed at elucidating and engineering their biosynthetic origin.[17]

Encouraged by the identified structural diversity of tetrapeptides, we set out to isolate the two major metabolites identified from the second MS^2 subnetwork (Figure 1D) and TIC, which were dominantly detectable within the 60% MeOH SPE fractions of culture extracts (Supporting Information). Again, MS-guided purification led to the isolation of analytically pure compound **5**, which was assigned the molecular formula $C_{22}H_{30}O_5N_2$ and nine degrees of unsaturation based on the ESI-HRMS mass spectrum (HRMS (ESI) *m/z*

$[M+H]^+$ calcd. for $C_{22}H_{31}O_5N_2^+$ 403.2228, found 403.2220, Δ_{ppm} −1.73) and acquired ^1H and ^{13}C NMR data (Table S6). The planar structure of **5** was first elucidated by a combined analysis of the 1D and 2D NMR spectra (Figure 3B). Interpretation of the ^1H and ^{13}C NMR spectra of **5** revealed three amide/ester carbonyl carbon signals [δ_C 172.0, 170.6, and 170.2] and two α-carbon/proton signals [δ_C 52.6; δ_H 4.74 and δ_C 48.7; δ_H 4.99] and one amide proton [δ_H 8.48] indicating typical features of a peptide-derived compound. A detailed 2D NMR analysis revealed that compound **5** was composed of two amino residues (Pro, Phe) and an additional 3,5-dihydroxy octanoic acid (DHOA). The ^1H,^{13}C two-bond coupling between NH [δ_H 8.48] of Phe and C-1 [δ_C 170.6] of DHOA implied the DHOA→Phe connectivity.

The β-proton of Pro [δ_H 3.44] exhibited heteronuclear correlation to C-1′ of Phe [δ_C 170.2] connecting the linkage between Phe and Pro. NOESY correlations from α- and β-protons [δ_H 4.74 and 2.85] of Phe to H-5″ [δ_H 3.16] of proline supported the connectivity of Phe to Pro. The sequence was accounted for 8 of the 9 degrees of unsaturation number (phenylalanine, proline ring, and three carbonyl signals). The remaining degree of unsaturation was deduced by correlation (HMBC) between the carbonyl carbon of Pro [δ_C 172.0] and methine proton [δ_H 4.66] of DHOA possessing an additional ring. Stereochemistry of the amino acids was first analyzed with Marfey's method using L-FDAA, which confirmed the presence of D-Phe and L-Pro. Finally, the relative (and absolute) structure was unambiguously solved by single X-ray analysis from a single crystal prepared in MeOH and H_2O (Figure 4). Again, following up on the MS^2-guided prediction, we isolated the second most dominant congener, compound **6** (HRMS (ESI) *m/z* $[M+H]^+$ calcd. for $C_{23}H_{33}O_5N_2^+$ 417.2384, found 417.2383, Δ_{ppm} −0.47). Comparative 1D and 2D NMR analysis revealed a similar core structure as **5**, but featuring an additional methyl group at C-2 [2-CH_3: δ_C 8.0; δ_H 0.81]. The stereochemistry of C-2 was determined based on NOESY correlations between NH of Phe [δ_H 8.46] and 2-H of DHOA [δ_H 2.57] with no correlation signal between NH [δ_H 8.46] and 2-CH_3 [δ_C 8.0] (Figure 3). The unexpected drastic upfield-shift of 2-CH_3 is potentially caused by direct orientation towards the aromatic ring of Phe and a strong ring current effect.

Based on their fungal origin and structural features, we named the polyketide- or fatty acid-NRPS-derived 12-membered macrocycles xylacremolide A (**5**) and B (**6**), respectively.

Following up on the identified structural features of compounds **5** and **6**, we reanalyzed the obtained MS^2 data and GNPS subnetwork and found that *Pseudoxylaria* sp. X187 presumably secretes also minor amounts of congeners that vary in the length and oxidation pattern of the PKS moiety (Supporting Information). However, low production titres prevented again further structure elucidation.

In general, xylacremolides share partial structural features with acremolides isolated from *Acremonium* sp.,[18] saroclides from the mangrove-derived fungus *Sarocladium kiliense* HDN11-112[19] and the fungus-derived histone deacetylase inhibitors FR235222[20] and trapoxin.[21] Here, it

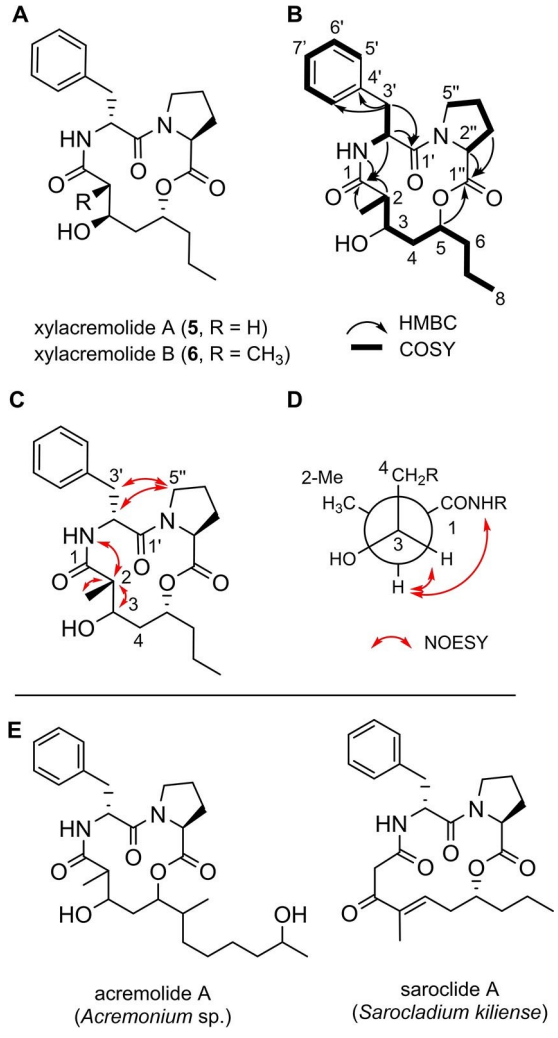

Figure 3. A) Structures of xylacremolide A (**5**) and B (**6**). B) Key COSY and HMBC, C) NOESY correlations and D) Newman projection of 2-Me (C2–C3 bond) to determine stereochemical assignment of **5** and **6**. E) Structures of related natural products.

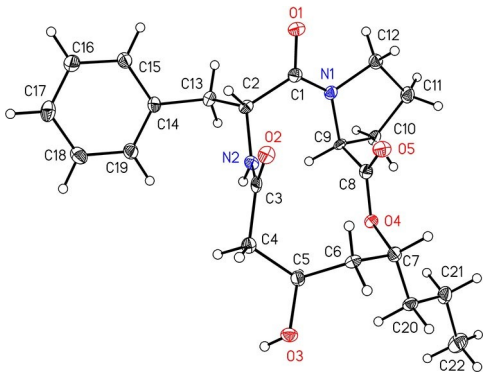

Figure 4. Crystal structure of xylacremolide A (**5**) shown as an ORTEP plot with displacement ellipsoids of non-hydrogen atoms drawn at the 50% probability level.

is important to note that xylacremolides, similar to acremolides and saroclide A, incorporate D-phenylalanine and L-proline, while FR235222 and trapoxin were reported to contain L-phenylalanine and D-proline.

However, the absolute structures of acremolides have so far not been reported. Similar as their structural counterparts, xylacremolides did not show cytotoxic, antibacterial or antifungal activities, which poses the intriguing question about the cellular or ecological role of these NRPS-PKS hybrids in *Pseudoxylaria* and other Ascomycota.

Conclusion

In summary, we selected *Pseudoxylaria* sp. X187 based on a phylogenetic and activity-guided approach for a detailed metabolomic investigation. HRMS^2-GNPS based analysis of guttation droplets and culture extracts from the aging fungal strain resulted in the identification of four linear N-acetylated and methylated peptides and two cyclic lipodepsipeptides. Although the reason for the active segregation of secondary metabolites into the guttation fluids remains speculative, the striking structural similarity amongst linear and cyclic tetrapeptides isolated from species across the Ascomycota division points towards a more general ecological or even cellular functions of this compound class.

Experimental Section

The Supporting Information contains all information regarding culture conditions, isolation procedures, structure elucidation, activity assays, ESI-HRMS, 1D and 2D NMR spectra, and crystallographic data.

Deposition number 1987814 (for **5**) contains the supplementary crystallographic data for this paper. These data are provided free of charge by the joint Cambridge Crystallographic Data Centre and Fachinformationszentrum Karlsruhe Access Structures service www.ccdc.cam.ac.uk/structures.

Acknowledgements

We are grateful for the financial support from the Deutsche Forschungsgemeinschaft (DFG) of this research project (BE 4799/3-1, CRC1127 project A6). We thank Heike Heinecke (Hans Knöll Institute) for recording the NMR spectra, Andrea Perner (Hans Knöll Institute) for HRMS measurements, Marius Faber, Christiane Weigel und Dr. Hans-Martin Dahse for activity assays. We thank Michael J. Wingfield, Bernard Slippers and the staff and students at the Forestry and Agricultural Biotechnology Institute (University of Pretoria) for supporting our research projects, and the Oerlemans family (Mookgophong) for permission to sample colonies at their farm.

Conflict of Interest

The authors declare no conflict of interest.

Keywords: metabolomics · natural products · nonribosomal peptide synthetase · peptides · polyketide synthases · symbionts

[1] U. G. Mueller, N. M. Gerardo, D. K. Aanen, D. L. Six, T. R. Schultz, *Annu. Rev. Ecol. Evol. Syst.* **2005**, *36*, 563–595.
[2] a) M. Poulsen, H. Hu, C. Li, Z. Chen, L. Xu, S. Otani, S. Nygaard, T. Nobre, S. Klaubauf, P. M. Schindler, F. Hauser, H. Pan, Z. Yang, A. S. M. Sonnenberg, Z. W. de Beer, Y. Zhang, M. J. Wingfield, C. J. P. Grimmelikhuijzen, R. P. de Vriese, J. Korb, D. K. Aanen, J. Wang, J. J. Boomsma, G. Zhang, *Proc. Natl. Acad. Sci. USA* **2014**, *111*, 14500–14505; b) S. Otani, V. L. Challinor, N. B. Kreuzenbeck, S. Kildgaard, S. Krath Christensen, L. L. M. Larsen, D. K. Aanen, S. A. Rasmussen, C. Beemelmanns, M. Poulsen, *Sci. Rep.* **2019**, *9*(1), 1–10.
[3] a) A. A. Visser, V. I. Ros, Z. W. de Beer, A. J. M. Debets, T. Hartog, T. W. Kuyper, T. Laessøe, B. Slippers, D. K. Aanen, *Mol. Ecol.* **2009**, *18*, 553–567; b) A. A. Visser, P. W. Kooij, A. J. M. Debets, T. W. Kuyper, D. K. Aanen, *Fungal Ecol.* **2011**, *4*, 322–332.
[4] a) H. Guo, N. B. Kreuzenbeck, S. Otani, M. Garcia-Altares, H. M. Dahse, C. Weigel, D. K. Aanen, C. Hertweck, M. Poulsen, C. Beemelmanns, *Org. Lett.* **2016**, *18*, 3338–3341; b) H. Guo, A. Schmidt, P. Stephan, L. Raguž, D. Braga, M. Kaiser, H. M. Dahse, C. Weigel, G. Lackner, C. Beemelmanns, *ChemBioChem* **2018**, *19*, 2307–2311.
[5] F. Song, S. H. Wu, Y. Z. Zhai, Q. C. Xuan, T. Wang, *Chem. Biodiversity* **2014**, *11*, 673–694.
[6] M. Wang, J. J. Carver, V. V. Phelan, L. M. Sanchez, N. Garg, Y. Peng, D. D. Nguyen, J. Watrous, C. A. Kapono, T. Luzzatto-Knaan, C. Porto, A. Bouslimani, A. V. Melnik, M. J. Meehan, W.-T. Liu, M. Crüsemann, P. D. Boudreau, E. Esquenazi, M. Sandoval-Calderón, R. D. Kersten, L. A. Pace, R. A. Quinn, K. R. Duncan, C.-C. Hsu, D. J. Floros, R. G. Gavilan, K. Kleigrewe, T. Northen, R. J. Dutton, D. Parrot, E. E. Carlson, B. Aigle, C. F. Michelsen, L. Jelsbak, C. Sohlenkamp, P. Pevzner, A. Edlund, J. McLean, J. Piel, B. T. Murphy, L. Gerwick, C.-C. Liaw, Y.-L. Yang, H.-U. Humpf, M. Maansson, R. A. Keyzers, A. C. Sims, A. R. Johnson, A. M. Sidebottom, B. E. Sedio, A. Klitgaard, C. B. Larson, C. A. Boya, P. D. Torres-Mendoza, D. J. Gonzalez, D. B. Silva, L. M. Marques, D. P. Demarque, E. Pociute, E. C. O'Neill, E. Briand, E. J. N. Helfrich, E. A. Granatosky, E. Glukhov, F. Ryffel, H. Houson, H. Mohimani, J. J. Kharbush, Y. Zeng, J. A. Vorholt, K. L. Kurita, P. Charusanti, K. L. McPhail, K. F. Nielsen, L. Vuong, M. Elfeki, M. F. Traxler, N. Engene, N. Koyama, O. B. Vining, R. Baric, R. R. Silva, S. J. Mascuch, S. Tomasi, S. Jenkins, V. Macherla, T. Hoffman, V. Agarwal, P. G. Williams, J. Dai, R. Neupane, J. Gurr, A. M. C. Rodríguez, A. Lamsa, C. Zhang, K. Dorrestein, B. M. Duggan, J. Almaliti, P.-M. Allard, P. Phapale, L.-F. Nothias, T. Alexandrov, M. Litaudon, J.-L. Wolfender, J. E. Kyle, T. O. Metz, T. Peryea, D.-T. Nguyen, D. VanLeer, P. Shinn, A. Jadhav, R. Müller, K. M. Waters, W. Shi, X. Liu, L. Zhang, R. Knight, P. R. Jensen, B. Ø. Palsson, K. Pogliano, R. G. Linington, M. Gutiérrez, N. P. Lopes, W. H. Gerwick, B. S. Moore, P. C. Dorrestein, N. Bandeira, *Nat. Biotechnol.* **2016**, *34*, 828–837.
[7] M. Gareis, C. Gottschalk, *Mycotoxin Res.* **2014**, *30*, 51–159.
[8] H. Laatsch, *Antibase Version 5.0—The Natural Compound Identifier*, Wiley-VCH, Weinheim, **2017**; ISBN: 978-3-527-34359-1.
[9] a) K. Fujii, Y. Ikai, H. Oka, M. Suzuki, K. I. Harada, *Anal. Chem.* **1997**, *69*, 5146–5151; b) S. Götze, P. Stallforth, *Org. Biomol. Chem.* **2020**, *18*, 1710–1727.
[10] K. Matsuda, T. Kuranaga, A. Sano, A. Ninomiya, K. Takada, T. Wakimoto, *Chef. Pharm. Bull.* **2019**, *67*, 476–480.
[11] N. S. Isaacs, *Physical Organic Chemistry*, 2nd ed., Longman Scientific and Technical: Harlow, **1995**, p 350.
[12] X. Liang, X. H. Nong, Z. H. Huang, S. H. Qi, *J. Agric. Food Chem.* **2017**, *65*, 5114–5121.
[13] J. Thongtan, J. Saenboonrueng, P. Rachtawee, M. Isaka, *J. Nat. Prod.* **2006**, *69*, 713–714.
[14] I. Pérez-Victoria, J. Martín, V. González-Menéndez, N. de Pedro, N. El Aouad, F. J. Ortiz-López, J. R. Tormo, G. Platas, F. Vicente, G. F. Bills, O. Genilloud, M. A. Goetz, F. Reyes, *J. Nat. Prod.* **2012**, *75*, 1210–1214.

[15] D. Schwarzer, R. Finking, M. A. Marahiel, *Nat. Prod. Rep.* **2003**, *20*, 275–287.
[16] H. Ali, M. I. Ries, P. P. Lankhorst, R. A. M. van der Hoeven, O. L. Schouten, M. Noga, T. Hankemeier, N. N. M. E. van Peij, R. A. L. Bovenberg, R. J. Vreeken, A. J. M. Driessen, *PLoS One* **2014**, *9*, e98212.
[17] M. Alanjary, C. Cano-Prieto, H. Gross, M. H. Medema, *Nat. Prod. Rep.* **2019**, *36*, 1249–1261.
[18] R. Ratnayake, L. J. Fremlin, E. Lacey, J. H. Gill, R. J. Capon, *J. Nat. Prod.* **2008**, *71*, 403–408.
[19] W. Guo, S. Wang, N. Li, F. Li, T. Zhu, Q. Gu, P. Guo, D. Li, *J. Nat. Prod.* **2018**, *81*, 1050–1054.
[20] H. Mori, Y. Urano, F. Abe, S. Furukawa, Y. Tsurumi, K. Sakamoto, M. Hashimoto, S. Takase, M. Hino, *J. Antibiot.* **2003**, *56*, 72–79.
[21] M. Kijima, M. Yoshida, K. Sugita, S. Horinouchi, T. Beppu, *J. Biol. Chem.* **1993**, *268*, 22429–22435.

Manuscript received: May 25, 2020
Accepted manuscript online: May 29, 2020
Version of record online: July 2, 2020